Chemical Research in Toxicology

ARTICLE

pubs.acs.org/crt

11-Oxoeicosatetraenoic Acid Is a Cyclooxygenase-2/15-Hydroxyprostaglandin Dehydrogenase-Derived Antiproliferative Eicosanoid

Xiaojing Liu,[†,‡] Suhong Zhang,[†] Jasbir S. Arora,[†] Nathaniel W. Snyder,[†] Sumit J. Shah,[†] and Ian A. Blair*[,†]

[†]Centers for Cancer Pharmacology and Excellence in Environmental Toxicology and [‡]Department of Chemistry, University of Pennsylvania, Philadelphia, Pennsylvania 19104-6160, United States

S Supporting Information

ABSTRACT: Previously, we established that 11(*R*)-hydroxy-5,8,12,14-(*Z*,*Z*,*E*,*Z*)-eicosatetraenoic acid (HETE) was a significant cyclooxygenase (COX)-2-derived arachidonic acid (AA) metabolite in epithelial cells. Stable isotope dilution chiral liquid chromatography (LC)-electron capture atmospheric pressure chemical ionization (ECAPCI)/mass spectrometry (MS) was used to quantify COX-2-derived eicosanoids in the human colorectal adenocarcinoma (LoVo) epithelial cell line, which expresses both COX-2 and 15-hydroxyprostaglandin dehydrogenase (15-PGDH). 11(*R*)-HETE secretion reached peak concentrations within minutes after AA addition before rapidly diminishing, suggesting further metabolism had occurred. Surprisingly, recombinant 15-PGDH, which is normally specific for oxidation of eicosanoid 15(*S*)-hydroxyl groups, was found to convert 11(*R*)-HETE to 11-oxo-5,8,12,14-(*Z*,*Z*,*E*,*Z*)-eicosatetraenoic acid (ETE). Furthermore, LoVo cell lysates converted 11(*R*)-HETE to 11-oxo-ETE and inhibition of 15-PGDH with 5-[[4-(ethoxycarbonyl)phenyl]azo]-2-hydroxy-benzeneacetic acid (CAY10397) (50 μM) significantly suppressed endogenous 11-oxo-ETE production with a corresponding increase in 11(*R*)-HETE. These data confirmed COX-2 and 15-PGDH as enzymes responsible for 11-oxo-ETE biosynthesis. Finally, addition of AA to the LoVo cells resulted in rapid secretion of 11-oxo-ETE into the media, reaching peak levels within 20 min of starting the incubation. This was followed by a sharp decrease in 11-oxo-ETE levels. Glutathione (GSH) *S*-transferase (GST) was found to metabolize 11-oxo-ETE to the 11-oxo-ETE-GSH (OEG)-adduct in LoVo cells, as confirmed by LC−MS/MS analysis. Bromodeoxyuridine (BrdU)-based cell proliferation assays in human umbilical vein endothelial cells (HUVECs) revealed that the half-maximal inhibitory concentration (IC_{50}) of 11-oxo-ETE for inhibition of HUVEC proliferation was 2.1 μM. These results show that 11-oxo-ETE is a novel COX-2/15-PGDH-derived eicosanoid, which inhibits endothelial cell proliferation with a potency that is similar to that observed for 15d-PGJ_2.

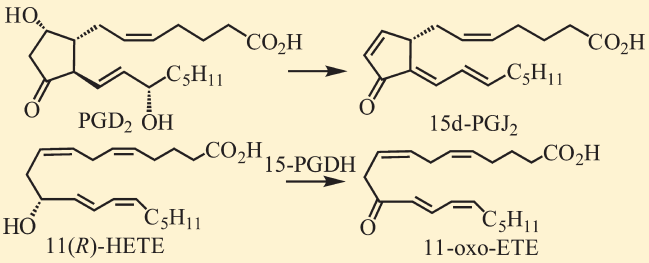

INTRODUCTION

In a previous study, we established that 11(*R*)-HETE was a significant COX-2-derived AA metabolite in epithelial cells.[1] However, the consequences of this finding were not clear at that time. A number of toxic substances including arsenite,[2] dioxin,[3] benzo[*a*]pyrene diol epoxide,[4] and cigarette smoke[5] upregulate COX-2 expression, which in turn regulates numerous intracellular biochemical pathways. This occurs primarily through the biosynthesis of COX-2-derived AA metabolites, which can exert cell-specific effects on inflammation, cell growth, and proliferation. For example COX-2-derived prostaglandin (PG) E_2 increases tumor proliferation through multiple mechanisms including activation of plasma membrane G-protein-coupled receptors and the nuclear peroxisome proliferator-activated receptor (PPAR)γ.[6]

Steady-state levels of PGE_2 are maintained by PGE-synthase-mediated biosynthesis from COX-2-derived PGH_2 and catabolism by 15-PGDH-mediated inactivation to 15-oxo-PGE_2 (Figure 1).[7,8] The 15-oxo-PGE_2 is then converted to 13,14-dihydro-15-oxo-PGE_2 by 15-oxoprostaglandin-Δ^{13} reductase.[9] Loss of 15-PGDH expression is associated with tumor formation in bladder, breast, colon, intestine, kidney, lung, pancreas, stomach, and skin cancer.[7,8,10−14] Thus, upregulation of COX-2[6] and downregulation of 15-PGDH[10] provides a switch toward endogenous mediators that are significant contributors to cancer progression.[15]

PGD_2, another COX-2-derived metabolite, is also metabolized by 15-PGDH to form 15-oxo-PGD_2, which is then converted to the corresponding inactive 13,14-dihydro derivative (Figure 1).[16] Alternatively, PGD_2 undergoes albumin-mediated dehydration to give PGJ_2, followed by a further dehydration to give 15-deoxy-$\Delta^{12,14}$-prostaglandin J_2 (15d-PGJ_2) (Figure 2).[17] Previous studies have shown that 15d-PGJ_2 is a PPARγ agonist,[18] which inhibits HUVEC proliferation in culture.[19] In addition, 15d-PGJ_2 can induce caspase-mediated endothelial cell apoptosis[20] and

Received: August 10, 2011
Published: September 14, 2011

 © 2011 American Chemical Society

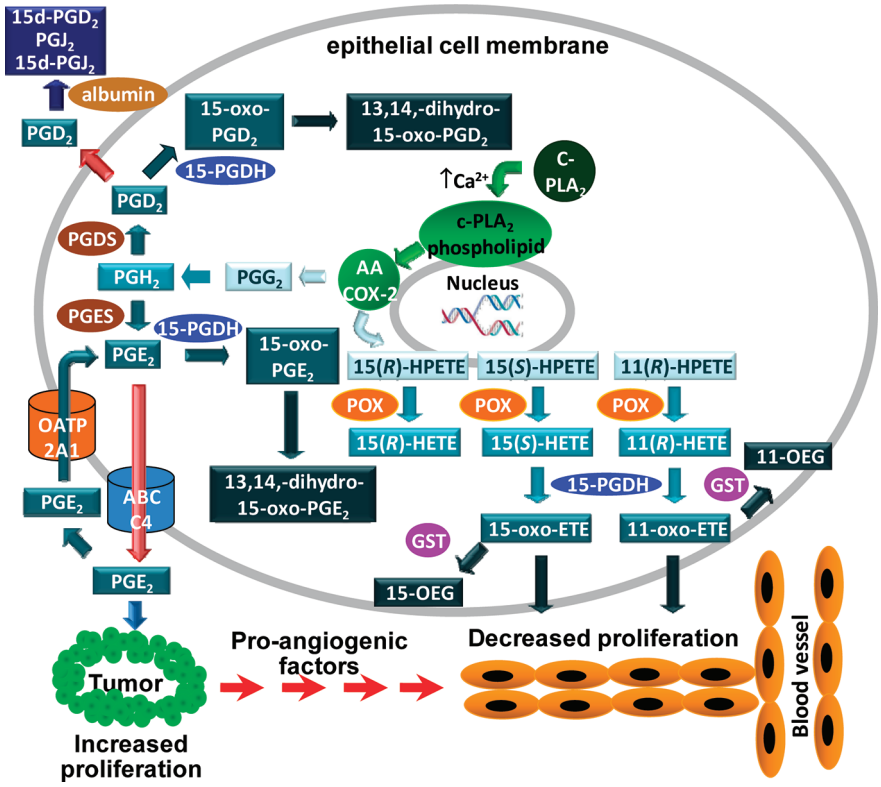

Figure 1. Formation and action of COX-2-derived eicosanoids in epithelial cell models. AA is released from membrane phospholipids by calcium-dependent cytosolic phospholipase A_2 ($cPLA_2$). The released AA undergoes COX-2-mediated metabolism to PGs or forms the lipid hydroperoxides, 15(*S*)-hydroperoxyeicosatetraenoic acid (HPETE), 15(*R*)-HPETE and 11(*R*)-HPETE, which are reduced to the corresponding HETEs. PGD_2 and PGE_2 are inactivated by 15-PGDH-mediated conversion to their 15-oxo metabolites. Both 15-oxo-PGD_2 and 15-oxo-PGE_2 are converted to 13,14-dihydro-5-oxo-PG metabolites. Intact PGD_2 secreted by the epithelial cells can undergo albumin-mediated dehydration to 15d-PGJ_2. PGE_2 secreted from the epithelial cells by the ABCC4 transporter is proproliferative for tumor cells. Reuptake of PGE_2 by OATP2A1 into the epithelial cells leads to further 15-PGDH-mediated inactivation. In contrast to PGE_2 and PGD_2, 15(*S*)-HETE and 11(*R*)-HETE are activated by 15-PGDH-mediated oxidation to 15-oxo-ETE and 11-oxo-ETE, respectively. The oxo-ETEs are further conjugated to form OEGs. Secreted 15- and 11-oxo-ETE that escape further metabolism can then inhibit endothelial cell proliferation. Therefore, downregulation of 15-PGDH and OATP2A1 would result in increased PGE_2-mediated tumor and endothelial cell proliferation.

inhibit the nuclear factor κB (NFκB) pathway.[21,22] It can also increase levels of p53 in HUVECs, activate p53 phosphorylation, and induce p21.[23]

Studies of purified COX enzymes have shown that 11(*R*)-HETE, 15(*S*)-hydroxy-5,8,11,13-(*Z*,*Z*,*Z*,*E*)-eicosatetraenoic acid (15(*S*)-HETE), and 15(*R*)-HETE are the major HETEs that are formed.[24] The HETEs arise from reduction of the corresponding hydroperoxyeicosatetraenoic acids (HPETEs) primarily through the peroxidase (POX) activity of COXs (Figure 1).[25] 11(*R*)-HETE was a significant eicosanoid secreted by AA-treated rat intestinal epithelial cells that stably express COX-2 (RIES cells), but it was rapidly metabolized.[1] 15(*S*)-HETE was formed in lower abundance and metabolized to 15-oxo-ETE,[24,26] as expected from its 15(*S*)-configuration and the substrate specificity of 15-PGDH. 15-Oxo-ETE was also found to inhibit endothelial cell proliferation, although at concentrations higher than 15d-PGJ_2.[26] However, there is little evidence that 15d-PGJ_2 can be formed *in vivo* at concentrations commensurate with an endogenous antiproliferative role.[27] In our earlier study,[1] the metabolic fate of 11(*R*)-HETE secreted by the RIES cells was not established. 11-Oxo-ETE has now been synthesized, and a LC-selected reaction monitoring (SRM)/MS method for its analysis has been developed. This has made it possible to determine whether 11-oxo-ETE is secreted by human epithelial cell lines with upregulated COX-2 expression and to identify the dehydrogenase responsible. The ability of 11-oxo-ETE to modulate HUVEC proliferation has also been examined.

EXPERIMENTAL PROCEDURES

Chemicals and Reagents. AA (peroxide-free), 11(*R*,*S*)-HETE, 15(*R*,*S*)-HETE, [$^2H_8$]-15(*S*)-HETE, [$^{13}C_{20}$]-15-oxo-ETE, 15-oxo-ETE, PGE_2, [$^2H_4$]-PGE_2, 13,14-dihydro-15-keto-PGE_2, [$^2H_4$]-13,14-dihydro-15-keto-PGE_2, 15d-PGJ_2, CAY10397, protease inhibitor cocktail and recombinant human 15-PGDH were purchased from Cayman (Ann Arbor, MI). The Dess−Martin reagent [1,1,1-tris(acetyloxy)-1,1-dihydro-1,2-benziodoxol-3-(1*H*)-one], 2,3,4,5,6-pentafluorobenzyl (PFB) bromide, Trizma-HCl, lipoxidase from *Glycine max* (soybean), sodium borohydride, and NAD^+ were purchased from Sigma-Aldrich (St. Louis, MO). Fetal bovine serum (FBS) was from Gemini Bioproducts (West Sacramento, CA). F12K medium, DMEM medium, Medium 200 (M200), D-glucose, L-glutamine, low-serum growth supplement (LSGS) kit, penicillin, and streptomycin were supplied by Invitrogen (Carlsbad, CA). LC−MS grade water, hexane, methanol, isopropanol, acetonitrile and dichloromethane were obtained from Fisher Scientific (Pittsburgh, PA). Gases were supplied by The Linde Group (Munich, Germany). [$^{13}C_{20}$]-AA was obtained from Spectra Stable Isotopes (Columbia, MD).

Cell Culture. Human colorectal adenocarcinoma LoVo cells (ATCC, Manassas, VA) were cultured in F12K medium supplemented with

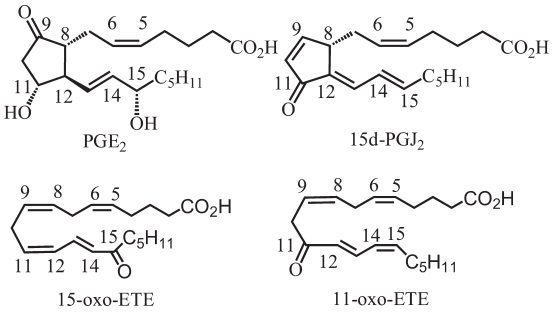

Figure 2. Chemical structures of COX-2-derived eicosanoids.

10% FBS, 2 mM L-glutamine, 100,000 units/L penicillin and 100 mg/L streptomycin. Human colonic adenocarcinoma HCA-7 Colony 29 cells (Sigma-Aldrich, St. Louis, MO) were grown in DMEM supplemented with 10% FBS, 2 mM L-glutamine, 110 mg/L sodium pyruvate, 100,000 units/L penicillin and 100 mg/L streptomycin. For lipidomics analysis, the culture medium was replaced with serum-free F12K or DMEM medium before the treatment. HUVECs were obtained from Invitrogen (Carlsbad, CA) and cultured on collagen I-coated tissue culture dishes in Medium 200 supplemented with LSGS kit. Cell proliferation assays were performed using HUVECs from passage 4.

Mass Spectrometry. A triple stage quadrupole (TSQ Quantum) mass spectrometer (Thermo Electron, San Jose, CA) equipped with an APCI source was used for the quantitative lipidomics analyses. Targeted chiral LC-ECAPCI/SRM/MS analysis was conducted using PFB derivatives of 7 lipids and 4 heavy isotope analogue internal standards. For the lipidomics profile, the instrument was operated in the negative ion mode, and unit resolution was maintained for both precursor and fragment ions. Operating conditions for the TSQ Quantum were as follows: vaporizer temperature at 450 °C; heated capillary temperature at 250 °C with the corona discharge needle set at 30 μA; nitrogen as sheath (25 psi) and auxiliary (5 arbitrary units) gas. Collision-induced dissociation (CID) was performed using argon as the collision gas at 2.7 mTorr in the rf-only quadrupole. The following SRM transitions were used: 11-oxo-ETE-PFB, m/z 317 → 165 (collision energy (CE), 25 eV); 15-oxo-ETE-PFB, m/z 317 → 113 (CE, 18 eV); [$^{13}C_{20}$]-15-oxo-ETE-PFB, m/z 337 → 120 (CE, 18 eV); 11(R)-HETE-PFB, m/z 319 → 167 (CE, 16 eV); [$^{2}H_{8}$]-15(S)-HETE-PFB, m/z 327 → 226 (CE, 13 eV); PGE_2-PFB, m/z 351 → 271 (CE, 18 eV); [$^{2}H_{4}$]-PGE_2-PFB, m/z 355 → 275 (CE, 18 eV); 13,14-dihydro-15-keto-PGE_2-PFB, m/z 351 → 235 (CE, 22 eV); [$^{2}H_{4}$]-13,14-dihydro-15-keto-PGE_2-PFB, m/z 355 → 239 (CE, 22 eV).

For GSH adduct analysis, the mass spectrometer was operated in the positive ion mode with an electrospray ionization (ESI) source. The operating conditions were as follows: spray voltage at 4 kV; capillary temperature at 350 °C; nitrogen as sheath (35 psi) and auxiliary (13 arbitrary units) gas. CID was performed using argon as the collision gas at 2.7 mTorr in the rf-only quadrupole. The following SRM transition (m/z 626 → 497) was monitored for 11-oxo-ETE-GSH (CE, 18 eV).

Liquid Chromatography. LC separations were conducted using a Waters Alliance 2690 HPLC system. A Chiralpak AD-H column (250 × 4.6 mm inner diameter, 5 μm; Daicel) was employed for normal phase separation (flow rate 1 mL/min) of PFB derivatives of eicosanoids. Gradient 1 was used for separating PFB-derivatives of HETEs and PGE_2, whereas gradient 2 was used for PFB derivatives of oxo-ETEs. For gradient 1, solvent A was hexane, and solvent B was methanol/isopropanol (1:1; v/v). Gradient 1 was as follows: 2% B at 0 min, 2% B at 3 min, 3.6% B at 11 min, 8% B at 15 min, 8% B at 27 min, 50% B at 30 min, 50% at 35 min, and 2% B at 37 min. Separations were performed at 30 °C using a linear gradient. For gradient 2, solvent A was hexane, and solvent B was isopropanol/hexane (6:4; v/v). Gradient 2 was as follows: 2% B at 0 min, 2% B at 14.5 min, 12% B at 15 min, 23% B at 19 min, 90% B at 19.5 min, 90% B at 23.5 min, and 2% B at 24 min.

A Chiralpak AD-RH column (150 × 4.6 mm inner diameter, 5 μm; Daicel) was used for reversed phase (isocratic method 1, flow rate 0.5 mL/min) separation of the underivatized 11-oxo-ETE. The mobile phase for isocratic separations was methanol/water/formic acid (95:5:0.1; v/v).

Chemically synthesized 11-oxo-ETE was purified by normal-phase (isocratic method 2) preparative LC (Ultrasphere 250 × 10 mm, inner diameter, 5 μm; Beckman) using Waters Alliance 2690 HPLC system by monitoring the UV absorbance at 236 nm. The mobile phase for the isocratic method 2 (flow rate 2.5 mL/min) was hexane/isopropanol/acetic acid (98.5:1.5:0.1 ; v/v).

GSH adducts were separated by reversed phase using gradient 3 on Waters Alliance 2690 HPLC system. The separation employed a Phenomenex Synergi Hydro-RP column (150 × 4.6 mm inner diameters, 5 μm). Solvent A was 0.1% aqueous formic acid, and solvent B was methanol/acetonitrile (50:50; v/v). Gradient 3 was as follows: 2% B at 0 min, 2% B at 14 min, 30% B at 20 min, 42% B at 21 min, 65% B at 27 min, 80% B at 29 min, 90% B at 33 min, 90% B at 34 min, 2% B at 35 min. The flow rate was 0.4 mL/min. The separation was performed at ambient temperature using a linear gradient.

PFB Derivatization. Eicosanoids were dissolved in 100 μL of acetonitrile and then reacted with 100 μL of PFB bromide in acetonitrile (1:19; v/v) and 100 μL of diisopropylethylamine in acetonitrile (1:9; v/v) at room temperature for 30 min. The derivatives were evaporated to dryness, dissolved in 100 μL of hexane/ethanol (95:5; v/v) and analyzed by chiral LC-ECAPCI/SRM/MS.

Enzymatic Conversion of 11(R)-HETE by 15-PGDH. Various concentrations of 11(R)-HETE (0, 2.3 μM, 4.6 μM, 6.9 μM, 9.2 μM and 23 μM) were incubated with 9 nM recombinant human 15-PGDH (52.2 ng, 1.8 pmol) and cofactor NAD^+ (400 μM) in 50 mM Tris-Cl (pH 7.9) for 3.5 min at 37 °C. Each total reaction volume was 200 μL. After a 3.5 min incubation, the enzymatic reaction was quenched with 400 μL of ice cold methanol and [$^{13}C_{20}$]-15-oxo-ETE (8 ng) added as the internal standard. Eicosanoids were extracted with 1.2 mL of dichloromethane/methanol (8:1; v/v). The lower organic layer was then evaporated to dryness under nitrogen and reconstituted in methanol (100 μL). An aliquot (25 μL) was separated using the isocratic method 1 and analyzed by LC−ESI/MS as described above. The retention time for 11-oxo-ETE was 8.7 min. In separate experiments, the formation of 11-oxo-ETE was found to be linear for the first 5 min. Eicosanoids were quantified by interpolation from a standard curve prepared with 11-oxo-ETE using [$^{13}C_{20}$]-15-oxo-ETE as the internal standard.

Chemical Synthesis and Purification of 11-Oxo-ETE. The Dess−Martin reagent (2 mg, 4.7 μmol) was added to a solution of 11(R,S)-HETE (0.5 mg, 1.6 μmol) in dichloromethane (1.0 mL) and stirred for 2 h at room temperature. The reaction was monitored by LC−MS using gradient 1 as described above, after PFB derivatization until there was no starting material left. There was only one major product, which corresponded to 11-oxo-ETE. The reaction mixture was centrifuged twice at 3,400 rpm (10 min), and the supernatant was evaporated. The residue was dissolved in the mobile phase (800 μL) and purified by isocratic method 2 as described above. The retention time for 11-oxo-ETE was 13.1 min. High resolution accurate mass measurements were obtained using electrospray ionization on a Thermo LTQ-FT mass spectrometer at a resolution of 100,000 (data not shown). NMR spectra were obtained on a Bruker 500 MHz NMR instrument.

15-PGDH Inhibition in LoVo or HCA-7 Cell Lysates by CAY10397. LoVo or HCA-7 cells were grown to 90% confluence, washed with 10 mL of phosphate-buffered saline (PBS) buffer (2 times), and then gently scraped in 600 μL of lysis buffer containing 0.1 M Tris-HCl (pH 7.9) and the protease inhibitor. Cell suspension was transferred to 2 mL Eppendorf tubes and sonicated for 60 s on ice (power 5).

Cell lysate was then incubated with or without the selective 15-PGDH inhibitor (CAY10397, 50 μM) and its cofactor (NAD^+, 500 μM) for 10 min at 37 °C. The pH was then adjusted to 4 with 10% aqueous acetic acid (10 μL) followed by addition of the internal standard mix, [$^{13}C_{20}$]-15-oxo-ETE, [$^2H_8$]-15(*S*)-HETE and [$^2H_4$]-PGE_2 (50 pg/μL, 20 μL). Diethyl ether (600 μL) was added, and samples were vortex-mixed and centrifuged (15000 rpm × 2 min). The organic layer was evaporated under nitrogen, and then the eicosanoids were derivatized with PFB bromide as mentioned above. Finally, samples were redissolved in hexane/ethanol (95:5; v/v, 100 μL) and analyzed (20 μL) by normal phase LC-ECAPCI/MS. The amounts of eicosanoids were normalized by protein concentrations of each lysate, which were determined by BCA assay.

Metabolism of AA by LoVo or HCA-7 Cells. LoVo or HCA-7 cells were grown to 90% confluence in 6-well plates as described above, and then fed fresh serum-free F-12K or DMEM medium. Cells were then incubated with AA (10 μM) for 0, 5, 10, and 30 min, 1 and 2.5 h at 37 °C. At each time point, 0.6 mL of medium was taken out, and 20 μL of 10% aqueous acetic acid was added to adjust pH to 3−4, together with 20 μL of internal standards mixture (50 pg/μL [$^{13}C_{20}$]-15-oxo-ETE, [$^2H_8$]-15(S)-HETE, [$^2H_4$]-PGE_2 and [$^2H_4$]-13,14-dihydro-15-keto-PGE_2-PFB). Then diethyl ether (1 mL) was added, and the mixture was vortex-mixed and centrifuged (15000 rpm × 2 min). The upper ether layer was evaporated under nitrogen, and PFB derivatives were synthesized as described above and analyzed by normal phase LC-ECAPCI/MS.

Standard Curves for Eicosanoid Quantification. To quantify eicosanoids excreted in the medium, Eppendorf tubes containing 0.6 mL of F12K medium were spiked with lipid standards, together with internal standards for [$^{13}C_{20}$]-15-oxo-ETE, [$^2H_8$]-15(S)-HETE, [$^2H_4$]-PGE_2 and [$^2H_4$]-13,14-dihydro-15-keto-PGE_2-PFB (1 ng each). To quantify eicosanoids in the cell lysate, lipid standards and internal standards mixture were spiked into 0.2 mL of Tris-HCl buffer. The extraction and PFB derivatization methods are the same as mentioned above.

Analysis of 11-OEG Adducts in LoVo cell Lysate. LoVo cells were grown to 90% confluence and then washed with PBS (10 mL). Cells were gently scraped in 600 μL of Tris-HCl buffer (0.1 M, pH = 7.9), containing protease inhibitor. Cell lysates were transferred to 2 mL Eppendorf tubes and sonicated for 60 s on ice (power 5). 11-Oxo-ETE (20 ng in ethanol) was added to the lysate together with 1 mM GSH. After incubation for 25 min at 37 °C, 10 μL of 10% acetic acid was added, and the sample was loaded onto an SPE column (Oasis HLB, 30 mg) preconditioned with methanol and then 0.1% formic acid. The column was washed with 1 mL of water and eluted with 250 μL of methanol, and then 20 μL was analyzed by reversed phase LC−ESI/MS using gradient 3, as described above.

Cell Proliferation Assay. BrdU incorporation in HUVECs was used to assess the effects of 11-oxo-ETE on cell proliferation. The BrdU assay was performed in a 96-well format using a commercially available colorimetric enzyme-linked immunosorbent assay (ELISA) kit (Roche), and also by immunofluorescence microscopy. Equal numbers of HUVECs in passage 4 were plated on either collagen-I coated 96-well plates (2000 cells/well) or collagen-I coated 8-chamber tissue culture glass slides (10000 cells/chamber). Cells were allowed to attach overnight in 0.25% DMSO containing medium. Eicosanoids were dissolved in DMSO, such that the final concentration of DMSO in cell medium was always 0.25% or lower. Cells were then treated for 24 h with either vehicle (0.25% DMSO), 11-oxo-ETE (1 nM to 100 μM), or 15d-PGJ_2 (1 nM to 100 μM). After 18 h of treatment, BrdU (final concentration, 10 μM in 0.25% DMSO) was added to each treatment group for an additional 6 h.

For the colorimetric ELISA, the manufacturer's protocol was followed to perform the assay. The absorbance at λ = 370 nm obtained from the assay was transformed to the cell numbers using a standard curve constructed by plating known number of HUVECs in triplicate. The IC_{50} values for eicosanoid inhibition of HUVEC proliferation were defined as the half maximal inhibitory concentration for endothelial cell proliferation over 24 h when compared with vehicle-treated cells. They were determined from the regression lines of the log inhibitor vs response curves using a least-squares fit.

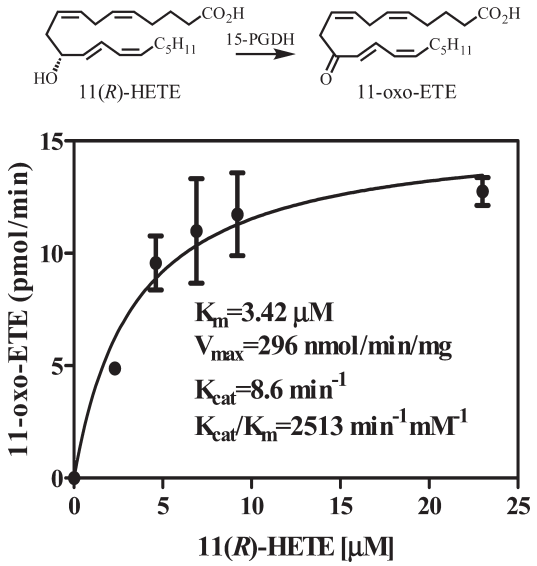

Figure 3. Kinetic plot of the formation of 11-oxo-ETE by 15-PGDH. Various concentrations of 11(*R*)-HETE (0−23 μM) were incubated with 9 nM recombinant 15-PGDH (52.2 ng, 1.8 pmol) and cofactor NAD^+. Determinations for 11-oxo-ETE were conducted in triplicate (means ± SEM) by stable isotope dilution LC−ESI/MS analyses.

For the immunofluorescence staining, cells were fixed with neutral buffered formalin for 10 min, permeabilized with methanol for 20 min, and then DNA was denatured by pressure cooking the slides in 10 mM citric acid buffer, pH 6 for 1 h. Cells were then incubated overnight with rat anti-BrdU antibody (1:1000, Accurate Chemical & Scientific Corp.) at 4 °C, followed by 30 min incubation at 37 °C with Cy3-conjugated donkey anti-rat secondary antibody (1:600, Jackson Immuno Research). Cells were counterstained with 4′,6-diamidino-2-phenylindole (DAPI, Invitrogen) and visualized using a Nikon E600 microscope equipped with differential interference contrast (Nomarski) optics and photographed (×200 magnification) with a Fast 1394 QICam (QImaging). Positive BrdU staining was quantified by image analysis using IVision Analysis Software (Biovision). The percentage of proliferating cells was determined by counting the BrdU-positive cells versus the total number of cells in randomly selected microscopic fields (10/replicate) for each treatment group.

Statistical Analyses. All experiments were conducted in triplicate, unless otherwise indicated. Statistical significance (p value ≤0.05) was determined using a two-tailed unpaired t test employing GraphPad Prism software (v 5.01).

RESULTS

Biosynthesis of 11-Oxo-ETE by 15-PGDH. Various concentrations of 11(*R*)-HETE were incubated with recombinant human 15-PGDH and NAD^+ at 37 °C. A Michaelis−Menten kinetic analysis of 11-oxo-ETE formation provided the V_{max} (296 nmol/min/mg of protein), K_m (3.42 μM), and k_{cat} (8.6 min^{-1}) values for oxidation of 11(*R*)-HETE (Figure 3) and the V_{max} (403.8 nmol/min/mg of protein, K_m (1.65 μM), and k_{cat} (8.6 min^{-1}) values for oxidation of 15(*S*)-HETE (Supplementary Figure 1 in the Supporting Information). Therefore, the catalytic efficiency (k_{cat}/K_m) for 15-PGDH-mediated oxidation of 11(*R*)-HETE (2513 min^{-1} mM^{-1}, Figure 3) was 35% of that found for

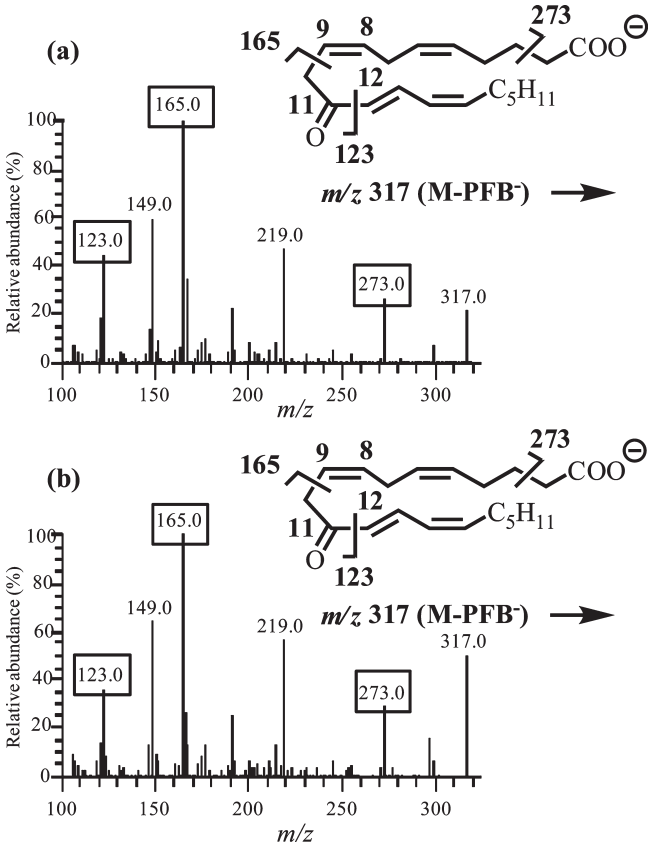

Figure 4. Confirmation of 11-oxo-ETE formation by LC−MS/MS analysis. Specific product ions observed by CID and MS/MS analysis of $[M\text{-}PFB]^{\bullet}$ (m/z 317), corresponding to 11-oxo-ETE are shown on the relevant chemical structures. (a) Synthetic 11-oxo-ETE-PFB standard; (b) 15-PGDH-derived 11-oxo-ETE-PFB from LoVo cell lysate to which 100 nM 11(R)-HETE had been added.

15(S)-HETE (7091 min^{-1} mM^{-1}; Supplementary Figure 1 in the Supporting Information).

Chemical Synthesis of Authentic 11-Oxo-ETE. 11-Oxo-ETE was synthesized chemically by oxidizing racemic 11(R,S)-HETE using the Dess−Martin reagent, and then purified using chromatographic separation. A combined total of 10 mg of the racemic 11(R,S)-HETE resulted in the isolation of 4.9 mg of pure 11-oxo-ETE (overall yield of 49%). High resolution electrospray ionization MS of 11-oxo-ETE revealed accurate masses of m/z 319.2263 and m/z 341.2079 for the protonated and sodiated molecules, respectively [calculated accurate mass for protonated ($C_{20}H_{31}O_3$) and sodiated ($C_{20}H_{30}O_3Na$) molecules, m/z 319.2273 and m/z 341.2093, respectively]. 500 MHz ^1H NMR (δH, $CDCl_3$; Supplementary Figure 2 in the Supporting Information): 7.55 (dd, J_1 = 11.5 Hz, J_2 = 15.5, 1H), 6.21(d, J =15.5 Hz, 1H), 6.15−6.11 (m, 1H), 5.97−5.92 (m, 1H), 5.60−5.58 (m, 2H), 5.41−5.38 (m, 2H), 3.35 (d, J = 4.5 Hz, 2H), 2.83−2.81 (m, 2H), 2.38−2.31 (m, 4H), 2.17−2.12 (m, 2H), 1.74−1.25 (m, 8H), 0.89 (t, J = 7.0 Hz, 3H). Analysis of purified 11-oxo-ETE as its PFB derivative by LC-ECAPCI/MS (Figure 4a) revealed an intense negative ion at m/z 317 corresponding to $[M - PFB]^-$. CID of $[M - PFB]^-$ (m/z 317) and MS/MS analysis revealed major product ions at m/z 273, 219, 165, 149, and 123. The UV spectrum was consistent with the presence of a conjugated dienone with a UV λ_{max} at 279 nm and molecular extinction coefficient (ε) of 18,985 M^{-1} cm^{-1}.

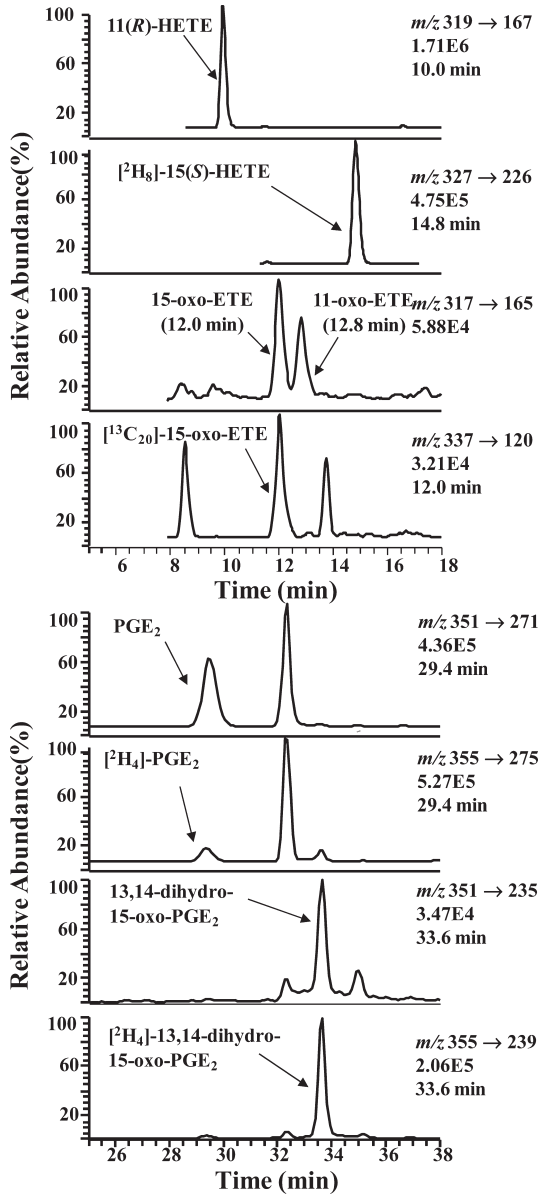

Figure 5. Targeted chiral lipidomics analysis of COX-2-derived eicosanoids from LoVo cells. LoVo cells were lysed; eicosanoids were extracted, derivatized with PFB bromide, and analyzed by LC-ECAP-CI/SRM/MS. LoVo cell lysates were pretreated with 50 μM CAY10397 to inhibit 15-PGDH to be able to detect the 11-, 15-HETEs and PGE_2. Representative chromatograms are shown for (top to bottom) (a) 11(R)-HETE-PFB (m/z 319 → 167), (b) $[^2H_8]$-15(S)-HETE-PFB internal standard (m/z 327 → 226), (c) 11-oxo-ETE-PFB (m/z 317 → 165) and 15-oxo-ETE-PFB (m/z 317 → 165), (d) $[^{13}C_{20}]$-15-oxo-ETE-PFB internal standard (m/z 337 → 120), (e) PGE_2-PFB (m/z 351 → 271), (f) $[^2H_4]$-PGE_2-PFB (m/z 355 → 275), (g) 13,14-dihydro-15-oxo-PGE_2-PFB (m/z 351 → 235), (h) $[^2H_4]$-13,14-dihydro-15-oxo-PGE_2-PFB (m/z 355 → 239).

Confirmation of 11-Oxo-ETE Identity by LC−MS and MS/MS Analyses. The LoVo cell line is known to express both COX-2 and 15-PGDH and only trace amounts of COX-1;[10,28] this was confirmed by Western blot analysis (data not shown). Cell lysates were incubated with 100 nM 11(R)-HETE in the presence of 500 μM NAD^+ for 10 min. LC−MS analysis of PFB derivatives of eicosanoids extracted from the LoVo cell lysate

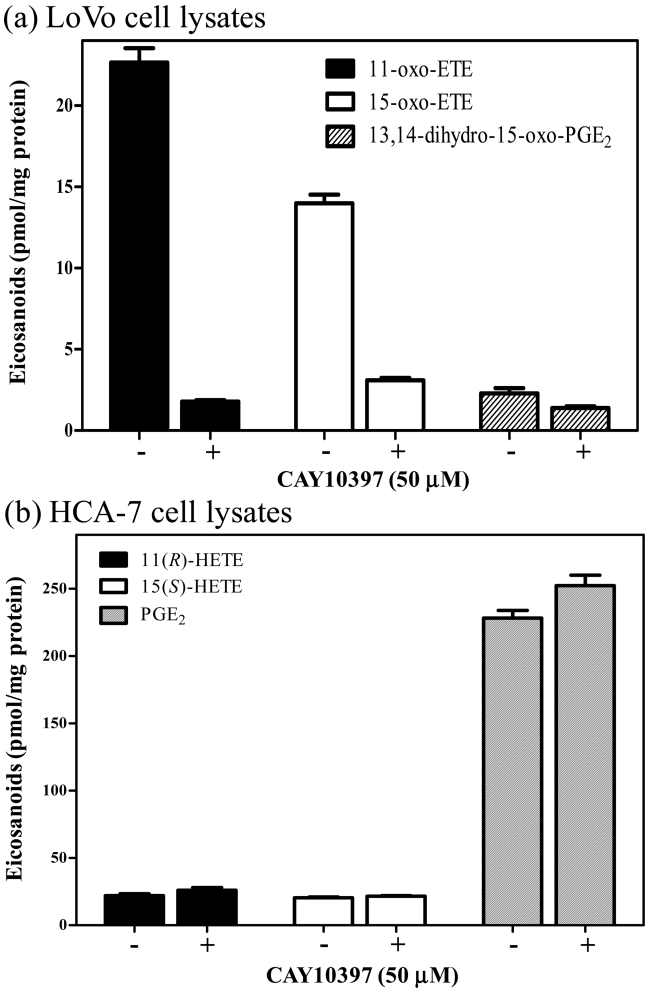

Figure 6. Inhibition of 15-PGDH in LoVo and HCA-7 cell lysates by CAY10397. (a) LoVo or (b) HCA-7 cell lysate (1×10^6 cells/treatment group) was incubated with or without CAY10397 (50 μM to inhibit 15-PGDH). Eicosanoids were extracted from the lysates, and their levels were determined by chiral LC-ECAPCI/SRM/MS. Analyses were performed in triplicate, and error bars show SEM.

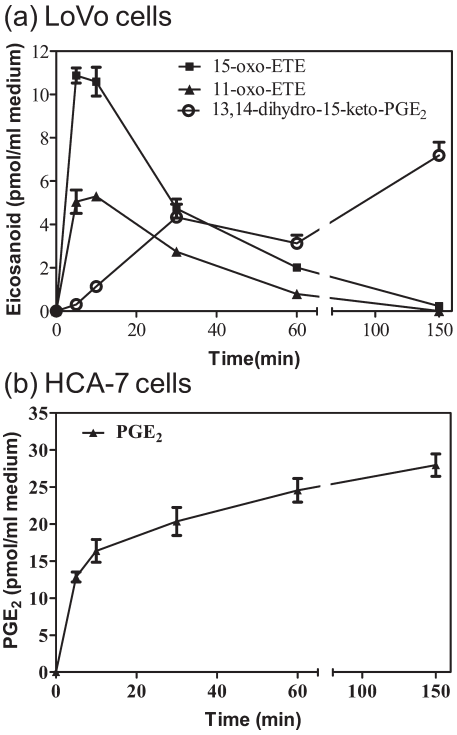

Figure 7. Time course for eicosanoids secreted from LoVo and HCA-7 cells following AA incubation. (a) LoVo or (b) HCA-7 cells were incubated with 10 μM AA for 0−6 h. The different eicosanoids secreted into the medium at various time points were extracted, and their levels were determined by stable isotope dilution LC-ECAPCI/SRM/MS analysis of their PFB derivatives. Determinations were conducted in triplicate (means ± SEM), and the quantitation was performed using the standard curves generated for these eicosanoids.

showed that there was a single major metabolite, which eluted at 12.8 min (data not shown). The full scan mass spectrum of this metabolite had only one major ion at m/z 317 corresponding to $[M - PFB]^-$ (Figure 4b). CID and MS/MS analysis revealed the formation of intense product ions at m/z 123, 149, 165, 219, and 273 (Figure 4b). The product ion spectrum was identical with that obtained from authentic synthetic 11-oxo-ETE-PFB (Figure 4a), which confirmed the identity of 11-oxo-ETE from LoVo cells. The product ion at m/z 165 in LoVo cell-derived and synthetic 11-oxo-ETE-PFB corresponded to cleavage between C-9 and C-10, and m/z 123 was formed from cleavage between C-11 and C-12 (Figure 4).

Separation of Eicosanoids by Chiral LC-ECAPCI/SRM/MS. Lysates from LoVo cells were extracted for the eicosanoids, which were then analyzed (after PFB derivatization) by LC-ECAPCI/SRM/MS. A representative chromatogram (Figure 5) reveals the separation of 11-oxo-ETE (retention time 12.8 min) and 15-oxo-ETE (retention time 12.0 min) that were formed in the LoVo cell lysate. Additional eicosanoids that were observed (Figure 5) include 13,14-dihydro-15-keto-PGE_2 (retention time, 33.6 min), 11(R)-HETE (retention time, 10.0 min), and PGE_2 (retention time, 29.4 min).

Inhibition of 15-PGDH by CAY10397 in LoVo and HCA-7 Cell Lysates. In contrast to LoVo cells, the HCA-7 cell line is known to express COX-2 and only trace amounts of COX-1 and 15-PGDH.[10,29] This was confirmed by Western blot analysis (data not shown). LoVo (Figure 6a) or HCA-7 (Figure 6b) cell lysates were incubated with 500 mM NAD^+, with or without the 15-PGDH inhibitor, CAY10397 (50 μM), for 10 min. Inhibition of 15-PGDH significantly abolished the formation of endogenous 11-oxo-ETE (Figure 6a) by 92%, along with the diminished formation of 15-oxo-ETE as well as 13,14-dihydro-15-oxo-PGE_2 (Figure 6a) in the LoVo cell lysate. However, since the oxo-ETEs and 13,14-dihydro-15-oxo-PGE_2 were undetectable in HCA-7 cell lysate, their precursors were quantified instead, and CAY10397 had no effect on their levels (Figure 6b).

Secretion of Eicosanoids from LoVo and HCA-7 Cells Following AA Addition. Time-course analyses for the amount of different eicosanoids secreted by LoVo and HCA-7 cells following AA incubation for 0−2.5 h are shown in Figure 7a and Figure 7b, respectively. 11-Oxo-ETE was secreted into the cell medium by LoVo cells along with 15-oxo-ETE and 13,14-dihydro-15-oxo-PGE_2 (Figure 7a). Interestingly, both 11-oxo-ETE and 15-oxo-ETE reached maximum concentrations 10 min after the addition of AA to the cells. This was followed by a decline of both eicosanoids to steady-state levels after 2.5 h (Figure 7a) in LoVo cells. In contrast, 13,14-dihydro-15-oxo-PGE_2

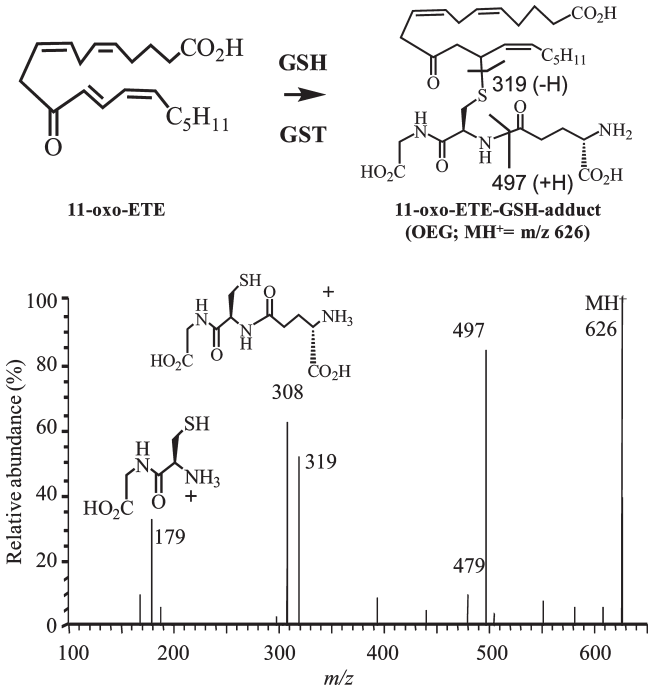

Figure 8. LC−MS/MS analysis of 11-OEG adduct. 11-OEG was synthesized by reacting 200 nM 11-oxo-ETE and 1 mM GSH in LoVo cell lysate for 25 min at 37 °C. The product was extracted by solid-phase extraction and analyzed by LC−ESI/MS/MS. Specific product ions observed by CID of $[MH]^+$ (m/z 626) are shown with their relevant chemical structures in the MS/MS analysis of 11-OEG.

levels did not peak until 1 h after the addition of AA (Figure 7a) and remained constant throughout the remainder of the incubation period. However, levels of the eicosanoids (11-oxo-ETE, 15-oxo-ETE or 13,14-dihydro-15-oxo-PGE_2) resulting from 15-PGDH-mediated metabolism were below detection limits in the medium of HCA-7 cells incubated with AA and, hence, are not displayed in Figure 7b. PGE_2 was secreted in the medium from HCA-7 cells incubated with AA (Figure 7b) demonstrating that the COX-2-mediated AA metabolism occurred. This ruled out the possibility that an artifact was responsible for lack of detection of 11-oxo-ETE, 15-oxo-ETE or 13,14-dihydro-15-oxo-PGE_2 in the HCA-7 cell media.

Formation of 11-OEG in LoVo Cell Lysates. Biosynthesis of 11-OEG was monitored in the cell lysate after the addition of 100 nM 11-oxo-ETE and 1 mM GSH to the LoVo cell lysate. 11-OEG formation was detected and confirmed by LC−MS/MS monitoring of the major metabolite formed after a 30 min incubation. OEG (retention time, 32.2 min, data not shown) was observed as an intense peak in the LC−ESI/MS chromatogram when analyzed by gradient 3 (as described above). CID and MS/MS analysis revealed the formation of intense product ions at m/z 497, 319, 308, and 179 (Figure 8).

Effects of Eicosanoids on HUVEC Proliferation. Proliferation by HUVECs was assessed by quantifying the BrdU incorporation into the cells actively synthesizing new DNA. The BrdU assay was performed using a quantitative colorimetric 96-well format ELISA as well as by immunofluorescence microscopy for observing the morphological effects of eicosanoids in HUVECs. For the BrdU ELISA, HUVECs (2000 cells/well) were treated with different doses (0−100 μM) of 11-oxo-ETE and 15d-PGJ_2 for a period of 24 h. The cell numbers corresponding to each

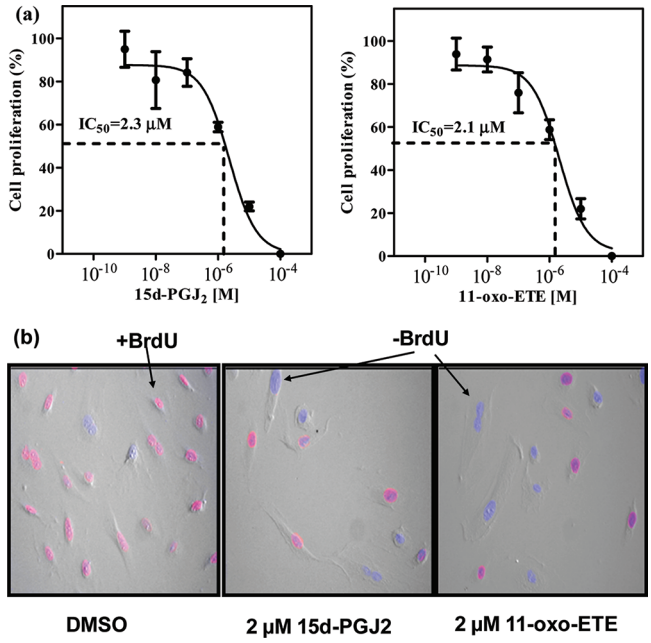

Figure 9. Effect of eicosanoids on cell proliferation of HUVECs. (a) For BrdU ELISA, HUVECs (2000 cells/well) were treated with various doses of 11-oxo-ETE and 15d-PGJ_2 for a period of 24 h. Cell proliferation (means ± SEM) was assessed by measuring absorbance at 370 nm and converting it to cell numbers using a standard curve and thereby used to construct the IC_{50} plots. All experiments were conducted three times in triplicate. Representative data from one experiment conducted in triplicate are shown as means ± SEM. (b) For immunofluorescence, HUVECs (8000/chamber) were treated with 2 μM 15d-PGJ_2 or 2 μM 11-oxo-ETE for 24 h and then stained for BrdU and counterstained with DAPI (cells stained blue). Photomicrographs were taken at ×200 magnification, and BrdU-positive (stained purple) cells were counted in randomly selected microscopic fields (10/replicate) as compared to the total number of cells in these fields. All experiments were conducted in triplicate. Representative photomicrographs from one set of replicates are shown.

treatment dose were computed and used to calculate cell proliferation (%) as compared to the vehicle-treated controls. 11-Oxo-ETE (IC_{50} = 2.1 μM) was equipotent with 15d-PGJ_2 (IC_{50} = 2.3 μM), a known potent inhibitor of endothelial cell proliferation (Figure 9a). For the immunofluorescence analysis, HUVECs (8000 cells/chamber) were treated with either 2 μM 11-oxo-ETE or 2 μM 15d-PGJ_2 for 24 h. BrdU incorporation was assessed by counting the BrdU-positive cells as compared to the total number of cells counted in randomly selected microscopic fields (10 fields/treatment). The photomicrographs clearly show that treatment with 11-oxo-ETE as well as 15d-PGJ_2 remarkably reduced the total number of BrdU-positive cells (stained red) as compared to vehicle-treated controls (Figure 9b). Moreover, there was a distinct change in the morphological appearance of the DAPI-stained (stained blue) cells in the eicosanoid-treated slides that failed to incorporate BrdU (Figure 9b).

DISCUSSION

15-PGDH catalyzes NAD^+-mediated oxidation of the 15(S)-hydroxyl moiety of PGs and other eicosanoids (Figure 1).[10,16,26] Our previous studies had established that 15-PGDH is also responsible for metabolizing the 15-lipoxygenase-derived 15(S)-HETE in macrophages and monocytes to 15-oxo-ETE.[26] Surprisingly, we have now found that 11(R)-HETE is also metabolized by

15-PGDH to a novel eicosanoid, that was identified as 11-oxo-ETE (Figure 2). The catalytic activity of human 15-PGDH for oxidation of 11(*R*)-HETE (Figure 2) was approximately one-third of that observed for 15(*S*)-HETE (Supplementary Figure 1 in the Supporting Information). These results were very surprising in view of the lack of a 15(*S*)-hydroxyl group on 11(*R*)-HETE as well as the incorrect 11(*R*)-stereochemistry. The structure of 11-oxo-ETE metabolite was established by chemically synthesizing authentic 11-oxo-ETE from racemic 11-HETE. 11-Oxo-ETE was formed in LoVo cell lysates (Figure 6a) and secreted from intact cells (Figure 7a); whereas 11-oxo-ETE was not formed by HCA-7 cell lysates (Figure 6b) or secreted from intact cells (Figure 7b). Since LoVo cells express COX-2 as well as 15-PGDH, whereas HCA-7 cells express COX-2 but not 15-PGDH,[10,28,29] these data convincingly prove that 11-oxo-ETE is an endogenous product formed enzymatically by a combination of COX-2 and 15-PGDH.

11-Oxo-ETE is isomeric with 15-oxo-ETE (Figure 2) and also has very similar LC properties. Therefore, a reversed phase LC-SRM/MS method was developed to separate the underivatized oxo-ETEs, and normal phase was implemented to separate their PFB derivatives. This made it possible to readily analyze the two oxo-ETEs. Endogenous eicosanoids formed by LoVo and HCA-7 epithelial cells and cell lysates as well as those formed after the addition of AA were analyzed as PFB derivatives by chiral LC-ECAPCI/MS.[30,31] Representative chromatograms of the eicosanoids produced endogenously in the LoVo cell lysates are shown in Figure 5. Inhibition of 15-PGDH enzyme by CAY10397 significantly diminished the formation of endogenous 11-oxo-ETE in LoVo cell lysates (Figure 6a). In addition, the formation of 15-oxo-ETE as well as 13,14-dihydro-15-oxo-PGE_2, the other two 15-PGDH-dependent metabolites, was also significantly reduced in LoVo cell lysates treated with CAY10397 (Figure 6a). In contrast, the three 15-PGDH products, namely, 11- and 15-oxo-ETE and 13,14-dihydro-15-oxo-PGE_2, were undetectable in HCA-7 cells as these cells do not express any 15-PGDH.[10,28] Instead, the corresponding precursors for these three metabolites were observed in the lysates. Furthermore, treatment with CAY10397 had no effect on levels of 11(*R*)-HETE, 15(*S*)-HETE or PGE_2 (Figure 6b). Intact LoVo cells also secreted 11-oxo-ETE and 15-oxo-ETE as well as 13,14-dihydro-15-oxo-PGE_2. However, the 11-oxo-ETE was cleared very rapidly (Figure 7a), suggesting that further metabolism was occurring. Subsequently, it was observed that 11-oxo-ETE underwent GSH conjugation to form 11-OEG, similar to the formation of 15-OEG in RIES cells (Figure 8).[1] GSH conjugation was predominantly catalyzed by the GST enzymes; however, it can also occur in a nonenzymatic manner. The relative amount of 11-OEG formed from these different pathways was not explored in detail in the present studies.

We realized that, despite its being a linear molecule, 11-oxo-ETE has structural similarities to the cyclopentenone eicosanoid 15d-PGJ_2 due to the presence of an 11-oxo moiety and a $\Delta^{12,14}$-diene (Figure 2). This suggested that 11-oxo-ETE might be a more effective inhibitor of HUVEC proliferation than 15-oxo-ETE[26] with a potency similar to that observed for 15d-PGJ_2.[19] In fact, 11-oxo-ETE was six times more potent than 15-oxo-ETE (data not shown) and equipotent with 15d-PGJ_2 at inhibition of HUVEC proliferation (Figure 9). Dose−response studies revealed that its IC_{50} was 2.1 μM compared to an IC_{50} value of 2.3 μM for 15d-PGJ_2 (Figure 9a). Moreover, immunofluorescence microscopy revealed that 11-oxo-ETE not only inhibited BrdU incorporation into the HUVECs but also caused a dramatic change in the shape and morphology of these cells (Figure 9b). Although the total number of cells counted in the eicosanoid-treated groups was quite similar to that in the vehicle-treated group, the BrdU-negative cells were significantly distorted (Figure 9b). Typically, if the cells are undergoing death by apoptosis, they would appear more compact and round. However, 11-oxo-treated cells were elongated and stretched (Figure 9b), which could be indicative of extensive cytoskeletal remodeling, cell cycle arrest and/or differentiation. Interestingly, 11-oxo-ETE formation could not be detected in HUVEC lysate that was incubated with 11(*R*)-HETE (data not shown). Furthermore, immunoblot analysis of HUVEC cell lysate failed to detect COX-2 protein (data not shown). Taken together, these data suggest a paracrine role for 11-oxo-ETE on endothelial cell proliferation.

As noted above, inhibition of 15-PGDH resulted in significant decreases in 11-oxo-ETE formation in LoVo cells (Figure 6). 15-PGDH is downregulated in numerous cancer types,[7,10−14] which would cause a decrease in 11-oxo-ETE biosynthesis by preventing the *in vivo* conversion of 11(*R*)-HETE to 11-oxo-ETE (Figure 1). This could be particularly devastating as COX-2 becomes upregulated during tumorigenesis, which would result in elevated PGE_2 biosynthesis along with decreased 15-PGDH-mediated inactivation to 15-oxo-PGE_2 (Figure 1). Ultimately, this would result in an increase in PGE_2-mediated proproliferative activity[6,15] without the counter effect of antiproliferative oxo-ETEs. Increased PGE_2 activity can also arise through downregulation of the influx PG transporter: the organic anion transporter polypeptide (OATP) 2A1 (Figure 1).[32,33] PGE_2 and 11-oxo-ETE can also arise from the metabolism of AA by constitutively expressed COX-1. Therefore, downregulation of 15-PGDH would also prevent the inactivation of COX-1-derived proproliferative PGE_2 as well as the biosynthesis of antiproliferative 11-oxo-ETE. These metabolic changes could also contribute to the eicosanoid-mediated effects that occur during tumorigenesis.

There is some evidence that 11-oxo-ETE can activate nuclear PPARγ.[34] PPARγ is a ligand-dependent transcription factor responsible for the regulation of a number of cellular events ranging from lipid metabolism to apoptosis.[35] 15d-PGJ_2 is a PPARγ agonist, which might account for its ability to inhibit endothelial cell proliferation.[18,19] However, this effect is only observed with pharmacological amounts of 15d-PGJ_2 rather than endogenous concentrations.[27] Besides PPARγ agonistic activity, 15d-PGJ_2 is also known to be an inhibitor of NFκB signaling, a pathway critical to cell proliferation as well as tumorigenesis.[36,37] In view of the ability of COX-2/15-PGDH to rapidly metabolize AA to nM amounts of oxo-ETEs, together with the similar structural features of the oxo-ETEs and 15d-PGJ_2 (Figure 2), it will be important to determine which of these activities are shared by both classes of eicosanoids. It is noteworthy that docosahexaenoic acid and docosapentaenoic acid can be metabolized by the sequential action of COX-2 and dehydrogenases into oxoeicosanoids that modulate the antioxidant response.[38] Similarly 5-lipoxygenase-derived 5(*S*)-HETE is metabolized by 5-hydroxyeicosanoid dehydrogenase into the chemoattractant 5-oxo-ETE.[39] Therefore, the oxoeicosanoids represent a family of oxidized lipids with diverse biological activities.

In summary, our studies have revealed that inhibition of 15-PGDH prevents the formation of endogenous antiproliferative eicosanoid, 11-oxo-ETE. Therefore, 15-PGDH has two quite distinct properties: it can either inactivate PGs or activate HETEs to oxo-ETEs that exert a paracrine effect on endothelial cells

(Figure 1). 11-Oxo-ETE, a member of the oxo-ETE family,[39−41] was observed previously as an endogenously derived lipid in human atherosclerotic plaques.[42] However, the biosynthesis of 11-oxo-ETE and its biological activity were not evaluated in that study. Furthermore, there does not appear to be any subsequent report of its formation either *in vitro* or *in vivo*. We have now shown that in fact 11-oxo-ETE is derived from COX-2/15-PGDH-mediated AA metabolism and that it inhibits endothelial cell proliferation with an IC_{50} that is very similar to that of 15d-PGJ_2.

■ ASSOCIATED CONTENT

Supporting Information. Kinetic plot of the formation of 15-oxo-ETE by 15-PGDH and 500 MHz ^{1}H NMR spectrum of 11-oxo-ETE in $CDCl^3$. This material is available free of charge via the Internet at http://pubs.acs.org.

■ AUTHOR INFORMATION

Corresponding Author

*Center for Cancer Pharmacology, University of Pennsylvania, 854 BRB II/III, 421 Curie Boulevard, Philadelphia, PA 19104-6160. Phone: 215-573-9885. Fax: 215-573-9889. E-mail: ianblair@mail.med.upenn.edu.

Funding Sources

This work was supported by the National Institutes of Health [RO1CA091016, UO1ES016004, P30ES013508, and P30-DK050306].

■ ACKNOWLEDGMENT

The authors would like to acknowledge Gary P. Swain at The Morphology Core of the Center for the Molecular Studies of Liver and Digestive Diseases, for his assistance with the BrdU immunofluorescence staining.

■ ABBREVIATIONS

11-HETE, 11-hydroxy-5,8,12,14-(*Z*,*Z*,*E*,*Z*)-eicosatetraenoic acid; 11-oxo-ETE, 11-oxo-5,8,12,14-(*Z*,*Z*,*E*,*Z*)-eicosatetraenoic acid; 15-HETE, 15-hydroxy-5,8,11,13-(*Z*,*Z*,*Z*,*E*)-eicosatetraenoic acid; 15-oxo-ETE, 15-oxo-5,8,11,13-(*Z*,*Z*,*Z*,*E*)-eicosatetraenoic acid; 15d-PGJ_2, 15-deoxy-$\Delta^{12,14}$-prostaglandin J_2; 15-PGDH, 15-hydroxyprostaglandin dehydrogenase; AA, arachidonic acid; ABC, ATP binding cassette; BrdU, 5-bromo-2-deoxyuridine; CAY10397, 5-[[4-(ethoxycarbonyl)phenyl]azo]-2-hydroxy-benzeneacetic acid; COX, cyclooxygenase; CID, collision-induced dissociation; $cPLA_2$, cytosolic phospholipase A_2; Dess−Martin reagent, [1,1,1-tris(acetyloxy)-1,1-dihydro-1,2-benziodoxol-3-(1*H*)-one]; ECAPCI, electron capture atmospheric pressure chemical ionization; ELISA, enzyme-linked immunosorbent assay; ESI, electrospray ionization; GSH, glutathione; GST, glutathione *S*-transferase; HPETE, hydroperoxyeicosatetraenoic acid; HUVEC, human umbilical vein endothelial cells; IC_{50}, half-maximal inhibitory concentration; LC, liquid chromatography; LSGS, low-serum growth supplement; MS, mass spectrometry; NSAID, nonsteroidal anti-inflammatory drug; OATP, organic anion transporter polypeptide; OEG, oxo-ETE-GSH adduct; PBS, phosphate-buffered saline; PG, prostaglandinPOX, peroxidase; PPAR, peroxisome proliferator-activated receptor; PFB, 2,3,4,5,6-pentafluorobenzyl bromide; RIES cells, rat intestinal epithelial cells stably expressing COX-2; SRM, selected reaction monitoring.

■ REFERENCES

(1) Lee, S. H., Rangiah, K., Williams, M. V., Wehr, A. Y., Dubois, R. N., and Blair, I. A. (2007) Cyclooxygenase-2-mediated metabolism of arachidonic acid to 15-oxo-eicosatetraenoic acid by rat intestinal epithelial cells. *Chem. Res. Toxicol. 20*, 665–1675.

(2) Ouyang, W., Zhang, D., Ma, Q., Li, J., and Huang, C. (2007) Cyclooxygenase-2 induction by arsenite through the IKKbeta/NFkappaB pathway exerts an antiapoptotic effect in mouse epidermal Cl41 cells. *Environ. Health Perspect. 115*, 513–518.

(3) Matsumura, F. (2009) The significance of the nongenomic pathway in mediating inflammatory signaling of the dioxin-activated Ah receptor to cause toxic effects. *Biochem. Pharmacol. 77*, 608–626.

(4) Ouyang, W., Ma, Q., Li, J., Zhang, D., Ding, J., Huang, Y., Xing, M. M., and Huang, C. (2007) Benzo[a]pyrene diol-epoxide (B[a]PDE) upregulates COX-2 expression through MAPKs/AP-1 and IKKbeta/NF-kappaB in mouse epidermal Cl41 cells. *Mol. Carcinog. 46*, 32–41.

(5) Huang, R. Y., and Chen, G. G. (2011) Cigarette smoking, cyclooxygenase-2 pathway and cancer. *Biochim. Biophys. Acta 1815*, 158–169.

(6) Wang, D., and Dubois, R. N. (2010) The role of COX-2 in intestinal inflammation and colorectal cancer. *Oncogene 29*, 781–788.

(7) Tai, H. H., Tong, M., and Ding, Y. (2007) 15-Hydroxyprostaglandin dehydrogenase (15-PGDH) and lung cancer. *Prostaglandins Other Lipid Mediat. 83*, 203–208.

(8) Hughes, D., Otani, T., Yang, P., Newman, R. A., Yantiss, R. K., Altorki, N. K., Port, J. L., Yan, M., Markowitz, S. D., Mazumdar, M., Tai, H. H., Subbaramaiah, K., and Dannenberg, A. J. (2008) NAD+-dependent 15-hydroxyprostaglandin dehydrogenase regulates levels of bioactive lipids in non-small cell lung cancer. *Cancer Prev. Res. 1*, 241–249.

(9) Chou, W. L., Chuang, L. M., Chou, C. C., Wang, A. H., Lawson, J. A., FitzGerald, G. A., and Chang, Z. F. (2007) Identification of a novel prostaglandin reductase reveals the involvement of prostaglandin E2 catabolism in regulation of peroxisome proliferator-activated receptor gamma activation. *J. Biol. Chem. 282*, 18162–18172.

(10) Backlund, M. G., Mann, J. R., Holla, V. R., Buchanan, F. G., Tai, H. H., Musiek, E. S., Milne, G. L., Katkuri, S., and Dubois, R. N. (2005) 15-Hydroxyprostaglandin dehydrogenase is down-regulated in colorectal cancer. *J. Biol. Chem. 280*, 3217–3223.

(11) Celis, J. E., Gromov, P., Cabezon, T., Moreira, J. M., Friis, E., Jirstrom, K., Llombart-Bosch, A., Timmermans-Wielenga, V., Rank, F., and Gromova, I. (2008) 15-prostaglandin dehydrogenase expression alone or in combination with ACSM1 defines a subgroup of the apocrine molecular subtype of breast carcinoma. *Mol. Cell. Proteomics 7*, 1795–1809.

(12) Pham, H., Chen, M., Li, A., King, J., Angst, E., Dawson, D. W., Park, J., Reber, H. A., Hines, O. J., and Eibl, G. (2010) Loss of 15-hydroxyprostaglandin dehydrogenase increases prostaglandin E2 in pancreatic tumors. *Pancreas 39*, 332–339.

(13) Thiel, A., Ganesan, A., Mrena, J., Junnila, S., Nykanen, A., Hemmes, A., Tai, H. H., Monni, O., Kokkola, A., Haglund, C., Petrova, T. V., and Ristimaki, A. (2009) 15-hydroxyprostaglandin dehydrogenase is down-regulated in gastric cancer. *Clin. Cancer Res. 15*, 4572–4580.

(14) Tseng-Rogenski, S., Gee, J., Ignatoski, K. W., Kunju, L. P., Bucheit, A., Kintner, H. J., Morris, D., Tallman, C., Evron, J., Wood, C. G., Grossman, H. B., Lee, C. T., and Liebert, M. (2010) Loss of 15-hydroxyprostaglandin dehydrogenase expression contributes to bladder cancer progression. *Am. J. Pathol. 176*, 1462–1468.

(15) Markowitz, S. D., and Bertagnolli, M. M. (2009) Molecular origins of cancer: Molecular basis of colorectal cancer. *N. Engl. J. Med. 361*, 2449–2460.

(16) Rangachari, P. K., and Betti, P. A. (1993) Biological activity of metabolites of PGD2 on canine proximal colon. *Am. J. Physiol. 264*, G886–G894.

(17) Fitzpatrick, F. A., and Wynalda, M. A. (1983) Albumin-catalyzed metabolism of prostaglandin D2. Identification of products formed in vitro. *J. Biol. Chem. 258*, 11713–11718.

(18) Forman, B. M., Tontonoz, P., Chen, J., Brun, R. P., Spiegelman, B. M., and Evans, R. M. (1995) 15-Deoxy-delta 12, 14-prostaglandin J2 is a ligand for the adipocyte determination factor PPAR gamma. *Cell 83*, 803–812.

(19) Xin, X., Yang, S., Kowalski, J., and Gerritsen, M. E. (1999) Peroxisome proliferator-activated receptor gamma ligands are potent inhibitors of angiogenesis in vitro and in vivo. *J. Biol. Chem. 274*, 9116–9121.

(20) Bishop-Bailey, D., and Hla, T. (1999) Endothelial cell apoptosis induced by the peroxisome proliferator-activated receptor (PPAR) ligand 15-deoxy-Delta12, 14-prostaglandin J2. *J. Biol. Chem. 274*, 17042–17048.

(21) Straus, D. S., Pascual, G., Li, M., Welch, J. S., Ricote, M., Hsiang, C. H., Sengchanthalangsy, L. L., Ghosh, G., and Glass, C. K. (2000) 15-deoxy-delta 12,14-prostaglandin J2 inhibits multiple steps in the NF-kappa B signaling pathway. *Proc. Natl. Acad. Sci. U.S.A. 97*, 4844–4849.

(22) Scher, J. U., and Pillinger, M. H. (2009) The anti-inflammatory effects of prostaglandins. *J. Invest. Med. 57*, 703–708.

(23) Ho, T. C., Chen, S. L., Yang, Y. C., Chen, C. Y., Feng, F. P., Hsieh, J. W., Cheng, H. C., and Tsao, Y. P. (2008) 15-deoxy-Delta-(12,14)-prostaglandin J2 induces vascular endothelial cell apoptosis through the sequential activation of MAPKS and p53. *J. Biol. Chem. 283*, 30273–30288.

(24) Lee, S. H., Williams, M. V., Dubois, R. N., and Blair, I. A. (2005) Cyclooxygenase-2-mediated DNA damage. *J. Biol. Chem. 280*, 28337–28346.

(25) Blair, I. A. (2008) DNA-adducts with lipid peroxidation products. *J. Biol. Chem. 283*, 15545–15549.

(26) Wei, C., Zhu, P., Shah, S. J., and Blair, I. A. (2009) 15-Oxo-Eicosatetraenoic Acid, a Metabolite of Macrophage 15-Hydroxyprostaglandin Dehydrogenase that Inhibits Endothelial Cell Proliferation. *Mol. Pharmacol. 76*, 516–529.

(27) Ide, T., Egan, K., Bell-Parikh, L. C., and FitzGerald, G. A. (2003) Activation of nuclear receptors by prostaglandins. *Thromb. Res. 110*, 311–315.

(28) Dixon, D. A., Tolley, N. D., King, P. H., Nabors, L. B., McIntyre, T. M., Zimmerman, G. A., and Prescott, S. M. (2001) Altered expression of the mRNA stability factor HuR promotes cyclooxygenase-2 expression in colon cancer cells. *J. Clin. Invest. 108*, 1657–1665.

(29) Shao, J., Sheng, H., Inoue, H., Morrow, J. D., and Dubois, R. N. (2000) Regulation of constitutive cyclooxygenase-2 expression in colon carcinoma cells. *J. Biol. Chem. 275*, 33951–33956.

(30) Lee, S. H., and Blair, I. A. (2007) Targeted chiral lipidomics analysis by liquid chromatography electron capture atmospheric pressure chemical ionization mass spectrometry (LC-ECAPCI/MS). *Methods Enzymol. 433*, 159–174.

(31) Mesaros, C., Lee, S. H., and Blair, I. A. (2009) Targeted quantitative analysis of eicosanoid lipids in biological samples using liquid chromatography-tandem mass spectrometry. *J. Chromatogr., B 877*, 2736–2745.

(32) Meijerman, I., Beijnen, J. H., and Schellens, J. H. (2008) Combined action and regulation of phase II enzymes and multidrug resistance proteins in multidrug resistance in cancer. *Cancer Treat. Rev. 34*, 505–520.

(33) Holla, V. R., Backlund, M. G., Yang, P., Newman, R. A., and Dubois, R. N. (2008) Regulation of prostaglandin transporters in colorectal neoplasia. *Cancer Prev. Res. 1*, 93–99.

(34) Waku, T., Shiraki, T., Oyama, T., Fujimoto, Y., Maebara, K., Kamiya, N., Jingami, H., and Morikawa, K. (2009) Structural insight into PPARgamma activation through covalent modification with endogenous fatty acids. *J. Mol. Biol. 385*, 188–199.

(35) Wang, D., and Dubois, R. N. (2008) Peroxisome proliferator-activated receptors and progression of colorectal cancer. *PPAR Res. 2008*, 931074.

(36) Ciucci, A., Gianferretti, P., Piva, R., Guyot, T., Snape, T. J., Roberts, S. M., and Santoro, M. G. (2006) Induction of apoptosis in estrogen receptor-negative breast cancer cells by natural and synthetic cyclopentenones: role of the IkappaB kinase/nuclear factor-kappaB pathway. *Mol. Pharmacol. 70*, 1812–1821.

(37) Piva, R., Gianferretti, P., Ciucci, A., Taulli, R., Belardo, G., and Santoro, M. G. (2005) 15-Deoxy-delta 12,14-prostaglandin J2 induces apoptosis in human malignant B cells: an effect associated with inhibition of NF-kappa B activity and down-regulation of antiapoptotic proteins. *Blood 105*, 1750–1758.

(38) Groeger, A. L., Cipollina, C., Cole, M. P., Woodcock, S. R., Bonacci, G., Rudolph, T. K., Rudolph, V., Freeman, B. A., and Schopfer, F. J. (2010) Cyclooxygenase-2 generates anti-inflammatory mediators from omega-3 fatty acids. *Nat. Chem. Biol. 6*, 433–441.

(39) Grant, G. E., Gravel, S., Guay, J., Patel, P., Mazer, B. D., Rokach, J., and Powell, W. S. (2011) 5-oxo-ETE is a major oxidative stress-induced arachidonate metabolite in B lymphocytes. *Free Radical Biol. Med. 50*, 1297–1304.

(40) O'Flaherty, J. T., Cordes, J. F., Lee, S. L., Samuel, M., and Thomas, M. J. (1994) Chemical and biological characterization of oxo-eicosatetraenoic acids. *Biochim. Biophys. Acta 1201*, 505–515.

(41) Grant, G. E., Rokach, J., and Powell, W. S. (2009) 5-Oxo-ETE and the OXE receptor. *Prostaglandins Other Lipid Mediators 89*, 98–104.

(42) Waddington, E., Sienuarine, K., Puddey, I., and Croft, K. (2001) Identification and quantitation of unique fatty acid oxidation products in human atherosclerotic plaque using high-performance liquid chromatography. *Anal. Biochem. 292*, 234–244.